PROCEEDINGS OF SCIENCE

Laser spectroscopy of long-lived pionic and antiprotonic helium in superfluid helium

M. Hori,[a,b,*] **H. Aghai-Khozani,**[a,1] **A. Sótér,**[a,2] **A. Dax,**[c] **D. Barna**[d,3] **and L. Venturelli**[e,f]

[a] *QUANTUM, Institut für Physik, Johannes Gutenberg-Universität Mainz, 55128 Mainz, Germany*
[b] *Max-Planck-Institut für Quantenoptik, Hans-Kopfermann-Strasse 1, D-85748 Garching, Germany*
[c] *Paul Scherrer Institut, Forschungsstrasse 111, CH-5232 Villigen, Switzerland*
[d] *CERN CH-1211, Geneva 23, Switzerland*
[e] *Dipartimento di Ingegneria dell'Informazione, Università di Brescia, Brescia, Italy*
[f] *Istituto Nazionale di Fisica Nucleare, Sezione di Pavia, Pavia, Italy*

E-mail: Masaki.Hori@cern.ch

The PiHe collaboration of PSI recently carried out laser spectroscopy of an infrared transition in three-body pionic helium atoms that were synthesized in a superfluid (He-II) helium target. Analogous measurements of antiprotonic helium atoms embedded in liquid helium were carried out by the ASACUSA collaboration of CERN. Spectral lines of unexpectedly narrow, sub-gigahertz linewidth were revealed in the antiproton case. An abrupt reduction in the linewidth was observed when the liquid helium (He-I) surrounding the atom transitioned into the superfluid phase.

41st International Conference on High Energy physics - ICHEP2022
6-13 July, 2022
Bologna, Italy

[1] Present address: McKinsey and Company, Sophienstrasse 26, 80333 Munich, Germany
[2] Present address: ETH Zürich, IPA, Otto-Stern-Weg 5, 8093 Zurich, Switzerland
[3] Present address: Institute for Particle and Nuclear Physics, Wigner Research Centre for Physics, H-1525 Budapest 114, P.O.B. 49, Hungary
[*] Speaker

PoS(ICHEP2022)141

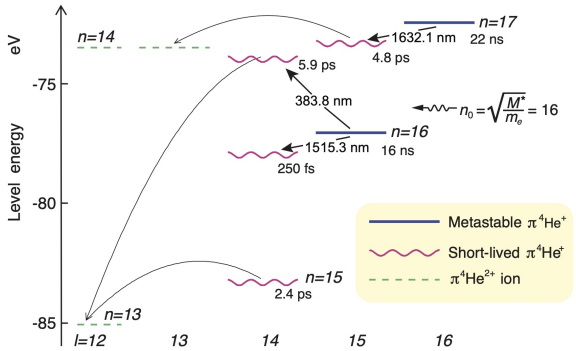

Figure 1: Energy level diagram of $\pi^4\mathrm{He}^+$ with the state energy (n, ℓ) plotted relative to the three-body breakup threshold. The wavy and solid lines indicate states with picosecond-scale and > 10 ns lifetime, respectively. The indicated state lifetimes include Auger, radiative, and weak decay rates. Dashed lines indicate the $\pi^4\mathrm{He}^{2+}$ ionic states, curved arrows some Auger transitions with multipolarity $\Delta\ell = 2$ [5].

1. Pionic helium

The PiHe collaboration carried out laser spectroscopy of three-body pionic helium atoms ($\pi^4\mathrm{He}^+ \equiv \pi^- + {}^4\mathrm{He}^{2+} + e^-$) [1–6] at the 590 MeV cyclotron facility of the Paul Scherrer Institute. This atom consists of a helium nucleus, an electron in the 1s ground state, and a π^- in a Rydberg state with principal and orbital angular momentum quantum numbers of $n \approx \ell + 1 \approx 17$ (see Fig. 1). The measurement corresponds to the first laser excitation of an atom containing a meson. The π^- mass M_π can be determined by comparing the experimental transition frequencies [4, 7, 8] with the results of QED calculations. The precision of the latter is now limited by the 10^{-6}-scale experimental uncertainty of M_π, but the relative precision of the calculations themselves is currently around 4×10^{-9} [6]. This should also help set upper limits on the laboratory constraints on the muon antineutrino mass [9], and exotic forces that may arise between the π^- and helium nucleus.

In the experiment, a π^- beam with a momentum 83–87 MeV/c and intensity of $(2-3) \times 10^7$ s^{-1} arrived at intervals of 19.75 ns and came to rest in a superfluid helium (He-II) target (Fig. 2 (a)). This produced $\pi^4\mathrm{He}^+$ atoms at a rate of $> 3 \times 10^5$ s^{-1} . An optical parameteric generator (OPG) and amplifier (OPA) (Fig. 2 (b)) were used to produce 800-ps long laser pulses of energy 10 mJ, repetition rate of 80.1 Hz, and wavelength of 1631 nm. The laser beam irradiated the atoms at a time $t = 9$ ns after π^- arrival. This excited a transition from the pionic state $(n, \ell) = (17, 16)$ with a nanosecond-scale lifetime, to a state $(17, 15)$ with a 5 ps Auger lifetime [4, 10, 11]. The two-body pionic helium ion ($\pi\mathrm{He}^{2+} \equiv \pi^- + \mathrm{He}^{2+}$) [12–15] that remained after Auger decay was destroyed by collisions with other helium atoms. The π^- was absorbed by the nucleus, and the emerging neutrons, protons, and deuterons with MeV-scale energies constituted the laser resonance signal. An array of plastic scintillators and waveform digitizers [16–19] measured the arrival time of these nuclear fragments.

The blue histogram of Fig. 3 (a) corresponds to the time spectrum of such arrivals measured without laser irradiation. The peaks at $t = 0$ and 19.75 ns arise from arrivals that led to immediate π^- absorption. A $(2.1 \pm 0.7)\%$ fraction of events corresponded to long-lived $\pi^4\mathrm{He}^+$ that decayed with a lifetime of (7 ± 2) ns in the intervals between the peaks. The spectrum represented by

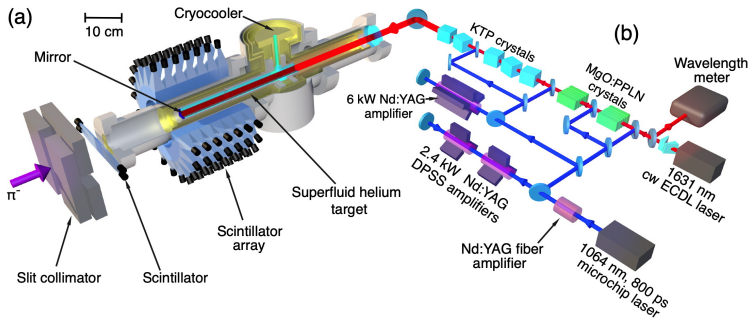

Figure 2: Layout of the πE5 experimental beamline used for laser spectroscopy of pionic helium atoms. (a): Schematic drawing of the experimental target. (b): Drawing of the laser system. From Ref. [5].

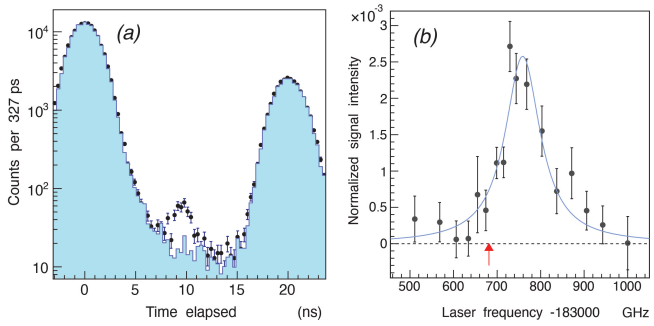

Figure 3: (a): Time spectra of nuclear fragments that emerged from π^- absorption by helium nuclei, measured with (indicated by filled circles) and without (blue histogram) the laser irradiation. The peak in the former spectrum at $t = 9$ ns corresponds to the laser resonance signal. (b): Spectral profile measured by scanning the laser frequency and plotting the signal counts. From Ref. [5].

filled circles was measured with the laser tuned to a wavelength of 1631.4 nm. The signal of the resonance $(17, 16) \rightarrow (17, 15)$ is seen at $t = 9$ ns.

Fig. 3 (b) shows the resonance profile measured by scanning the laser frequency and accumulating data over a period of a few weeks. The resonance width of $\approx$ 100 GHz mostly arises from the Auger width $\Gamma_A = 33$ GHz of the daughter state $(17, 15)$ [4, 11], and from collisional [2] and power broadening, and the laser linewidth. Atomic collisions in the He-II target may shorten [1, 20, 21] the state lifetimes and cause additional broadening. The blue curve shows the result of the best fit of two overlapping Lorentzian functions that represent the hyperfine sublines due to the interaction between the electron spin and orbital angular momentum. From this the resonance centroid was determined as $\nu_{\rm exp} = 183760(6)(6)$ GHz, with a statistical uncertainty of 6 GHz, and systematic uncertainty of 6 GHz. The latter contains contributions from the choice of the fit function and the uncertainty of the laser frequency. The experimental frequency $\nu_{\rm exp}$ is larger than the theoretical value $\nu_{\rm th} = (183681.8 \pm 0.5)$ GHz obtained from QED calculations [4]. The impact approximation of the binary collision theory of spectral lineshapes [2] predicts a frequency shift of between $\Delta\nu = 96$ and 142 GHz due to atomic collisions in the experimental target [1, 2, 20, 22–24]. This shift is in rough agreement with the experimental data. We plan to next search for transitions that are narrower by a factor of at least 10^{-3} compared to the above resonance. Pionic atoms may also be produced at the gamma factory proposed at CERN [25].

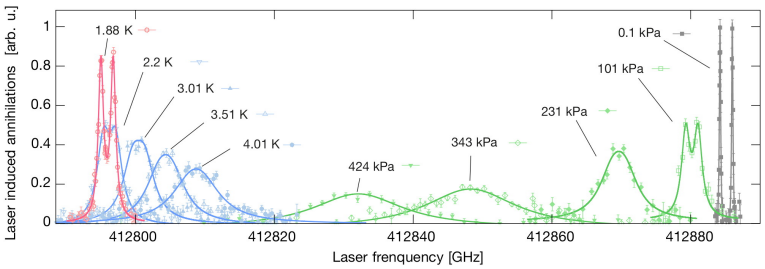

Figure 4: Spectral lines of $\overline{p}^4\mathrm{He}^+$ measured in gaseous and supercritical helium (green data points), He-I (blue) and He-II (red) targets. From Ref. [24].

2. Antiprotonic helium in superfluid helium

The ASACUSA collaboration has carried out laser spectroscopy of antiprotonic helium atoms ($\overline{p}\mathrm{He}^+ \equiv \overline{p}+\mathrm{He}^{2+}+e^-$) using the Antiproton Decelerator (AD) of CERN [23, 24, 26–37]. This atom contains an antiproton in a Rydberg state with quantum numbers of $n \approx \ell+1 \approx 38$ [21, 34, 38]. The atom constitutes the hadron-antihadron bound system with the longest, microsecond-scale lifetime that can be readily produced. Sub-Doppler two-photon laser spectroscopy [33, 39] and buffer gas cooling of the atom [36] have been utilized to measure its transition frequencies with parts-per-billion scale precision. By comparing the experimental frequencies with the results of QED calculations [26, 27], the antiproton-to-electron mass ratio was determined as $M_{\overline{p}}/m_e = 1836.1526734(15)$ [36]. This agreed with the proton-to-electron value. The results were also used to set upper limits on fifth forces involving antiprotons at atomic length scales [31, 40, 41], and on hypothetical spin-dependent forces that may arise between an electron and antiproton mediated by spin=0 or 1 bosons such as axions [42]. The new ELENA facility [43] provides an antiproton beam of kinetic energy $E = 100$ keV and an emittance of a few π mm·mrad. This beam will be used to search for transitions with natural widths two orders of magnitude narrower than the ones measured so far [39]. This may allow us to study QED and CPT symmetry at parts-per-trillion scale precision.

We recently observed an unexpected behaviour of $\overline{p}^4\mathrm{He}^+$ atoms embedded in He-I and He-II targets. A radiofrequency quadrupole decelerator (RFQD) [44] slowed down a beam of antiprotons to a kinetic energy between $E = 3.2$ and 5.3 MeV. The $\overline{p}^4\mathrm{He}^+$ atoms were synthesized by allowing the antiprotons to come to rest in either a gaseous or liquid helium (He-I) target. The beamline was also used to study the cross sections of antiprotons annihilating in some target foils [18, 19, 45–50]. The $\overline{p}\mathrm{He}^+$ atoms were irradiated by nanosecond laser pulses [51] which excited the transitions $(n,\ell) = (39,35)\rightarrow(38,34)$ and $(37,35)\rightarrow(38,34)$. The resonance condition was resolved as a spike in the rate of the resulting antiproton annihilations measured by a Cherenkov detector [16].

Fig. 4 (green data points) shows the spectral lines measured in gaseous and supercritical helium at pressures $p = 101$–424 kPa and temperature T= 6.0–6.4 K. As the target density was increased, progressively larger collisional shifts and broadenings relative to the spectra of $p = 0.1$ kPa and $T \approx 1.6$ K (grey) were observed. The spectra in He-I targets (blue) became unexpectedly narrower as the liquid temperature was reduced. A rapid reduction of the linewidth below the He-II (red) transition temperature revealed the hyperfine structure arising from the spin-spin interaction between the antiproton and electron. The reason for this effect is not understood and currently being

theoretically studied.

This work was supported by DFG (project 498537483).

References

[1] V.I. Korobov et al., *J. Phys. B* **48** (2015) 245006.

[2] B. Obreshkov, D. Bakalov, *Phys. Rev. A* **93** (2016) 062505.

[3] D. Baye, J. Dohet-Eraly, *Phys. Rev. A* **103** (2021) 022823.

[4] M. Hori, A. Sótér, V.I. Korobov, *Phys. Rev. A* **89** (2014) 042515.

[5] M. Hori, H. Aghai-Khozani, A. Sótér, A. Dax, D. Barna, *Nature* **581** (2020) 37.

[6] Z.-D. Bai et al., *Phys. Rev. Lett.* **128** (2022) 183001.

[7] M. Trassinelli et al., *Phys. Lett. B* **759** (2016) 583.

[8] M. Daum, R. Frosch, P.-R. Kettle, *Phys. Lett. B* **796** (2019) 11.

[9] K. Assamagan et al., *Phys. Rev. D* **53** (1996) 6065.

[10] H. Yamaguchi et al., *Phys. Rev. A* **66** (2002) 022504.

[11] H. Yamaguchi et al., *Phys. Rev. A* **70** (2004) 012501.

[12] M. Hori et al., *Phys. Rev. Lett.* **94** (2005) 063401.

[13] J. Zatorski, K. Pachucki, *Phys. Rev. A* **82** (2010) 052520.

[14] J. Zatorski, V. Patkóš, K. Pachucki, *Phys. Rev. A* **106** (2022) 042804.

[15] G.Y. Korenman, S.N. Yudin, *Eur. Phys. J. D* **75** (2021) 64.

[16] M. Hori, K. Yamashita, R. Hayano, T. Yamazaki, *Nucl. Instr. and Meth. A* **496** (2003) 102.

[17] A. Sótér et al., *Rev. Sci. Instrum.* **85** (2014) 023302.

[18] K. Todoroki et al., *Nucl. Instr. and Meth. A* **835** (2016) 110.

[19] Y. Murakami, H. Aghai-Khozani, M. Hori, *Nucl. Instrum. and Meth. A* **933** (2019) 75.

[20] M. Hori et al., *Phys. Rev. Lett.* **87** (2001) 093401.

[21] M. Hori et al., *Phys. Rev. A* **70** (2004) 012504.

[22] D. Bakalov et al., *Phys. Rev. Lett.* **84** (2000) 2350.

[23] A. Adamczak, D. Bakalov, *Phys. Rev. A* **88** (2013) 042505.

[24] A. Sótér et al., *Nature* **603** (2022) 411.

[25] V.V. Flambaum, J. Jin, D. Budker, *Phys. Rev. C* **103** (2021) 054603.

[26] V.I. Korobov, L. Hilico, J.-P. Karr, *Phys. Rev. Lett.* **112** (2014) 103003.

[27] V.I. Korobov, *Phys. Rev. A* **89** (2014) 014501.

[28] K. Sakimoto, *Phys. Rev. A* **91** (2015) 042502.

[29] M.-H. Hu et al., *Chem. Phys. Lett.* **654** (2016) 114.

[30] Z.-D. Bai, Z.-X. Zhong, Z.-C. Yan, T.-Y. Shi, *Chin. Phys. B* **30** (2021) 023101.

[31] M. Germann et al., *Phys. Rev. Research* **3** (2021) L022028.

[32] M. Hori et al., *Phys. Rev. Lett.* **96** (2006) 243401.

[33] M. Hori et al., *Nature* **475** (2011) 484.

[34] T. Kobayashi et al., *J. Phys. B* **46** (2013) 245004.

[35] S. Friedreich et al., *J. Phys. B* **46** (2013) 125003.

[36] M. Hori et al., *Science* **354** (2016) 610.

[37] M. Hori, J. Walz, *Prog. Part. Nucl. Phys.* **72** (2013) 206.

[38] M. Hori et al., *Phys. Rev. Lett.* **89** (2002) 093401.

[39] M. Hori, V.I. Korobov, *Phys. Rev. A* **81** (2010) 062508.

[40] E. Salumbides, W. Ubachs, V.I. Korobov, *J. Mol. Spectrosc.* **300** (2014) 65.

[41] J. Murata, S. Tanaka, *Class. Quantum Gravity* **32** (2015) 033001.

[42] F. Ficek et al., *Phys. Rev. Lett.* **120** (2018) 183002.

[43] V. Chohan et al., *CERN-2014-002, Geneva, Switzerland* (2014) .

[44] M. Hori et al., *Phys. Rev. Lett.* **91** (2003) 123401.

[45] A. Bianconi et al., *Phys. Lett. B* **704** (2011) 461.

[46] H. Aghai-Khozani et al., *Eur. Phys. J. Plus* **127** (2012) 125.

[47] M. Corradini et al., *Nucl. Instrum. and Meth. A* **711** (2013) 12.

[48] H. Aghai-Khozani et al., *Nucl. Phys. A* **970** (2018) 366.

[49] H. Aghai-Khozani et al., *Nucl. Phys. A* **1009** (2021) 122170.

[50] K. Nordlund, M. Hori, D. Sundholm, *Phys. Rev. A* **106** (2022) 012803.

[51] M. Hori, A. Dax, *Opt. Lett.* **34** (2009) 1273.